Identifying potential areas of Cannabis sativa plantations using object-based image analysis of SPOT-5 satellite data

Alessandra Lisita [a] , Edson E. Sano [b] & Laurent Durieux [c]

[a] Departamento de Polícia Federal, Instituto Nacional de Criminalística , Área de Perícias de Meio Ambiente , Brasília , DF , Brazil

[b] Empresa Brasileira de Pesquisa Agropecuária , Planaltina , DF , Brazil

[c] Institut de Recherche pour le Développement (IRD), UMR 228 ESPACE-DEV – Maison de la Télédétection , Montpellier Cedex , 05, 34093 , France
Published online: 22 Apr 2013.

PLEASE SCROLL DOWN FOR ARTICLE

demand, or costs or damages whatsoever or howsoever caused arising directly or indirectly in connection with or arising out of the use of this material.

Taylor & Francis
Taylor & Francis Group

Identifying potential areas of *Cannabis sativa* plantations using object-based image analysis of SPOT-5 satellite data

Alessandra Lisita[a]*, Edson E. Sano[b], and Laurent Durieux[c]

[a]Departamento de Polícia Federal, Instituto Nacional de Criminalística, Área de Perícias de Meio Ambiente, Brasília, DF Brazil; [b]Empresa Brasileira de Pesquisa Agropecuária, Planaltina, DF Brazil; [c]Institut de Recherche pour le Développement (IRD), UMR 228 ESPACE-DEV – Maison de la Télédétection, Montpellier Cedex 05, 34093, France

The rapid and efficient detection of illicit drug cultivation, such as that of *Cannabis sativa*, is important in reducing consumption. The objective of this study was to identify potential sites of illicit *C. sativa* plantations located in the semi-arid, southern part of Pernambuco State, Brazil. The study was conducted using an object-based image analysis (OBIA) of Système Pour l'Observation de la Terre high-resolution geometric (SPOT-5 HRG) images (overpass: 31 May, 2007). OBIA considers the target's contextual and geometrical attributes to overcome the difficulties inherent in detecting illicit crops associated with the grower's strategies to conceal their fields and optimizes the spectral information extracted to generate land-cover maps. The capabilities of the SPOT-5 near-infrared and shortwave infrared bands to discriminate herbaceous vegetation with high water content, and employment of the support vector machine classifier, contributed to accomplishing this task. Image classification included multiresolution segmentation with an algorithm available in the eCognition Developer software package. In addition to a SPOT-5 HRG multispectral image with 10 m spatial resolution and a panchromatic image with 2.5 m spatial resolution, first-order indices such as the normalized difference vegetation index and ancillary data including land-cover classes, anthropogenic areas, slope, and distance to water sources were also employed in the OBIA. The classification of segments (objects) related to illegal cultivation employed fuzzy logic and fixed-threshold membership functions to describe the following spectral, geometrical, and contextual properties of targets: vegetation density, topography, neighbourhood, and presence of water supplies for irrigation. The results of OBIA were verified from a weight of evidence analysis. Among 15 previously known *C. sativa* sites identified during police operations conducted on 5–17 June 2007, eight sites were classified as maximum-alert areas (total area of 22.54 km^2 within a total area of object-oriented image classification of ∼1800 km^2). The approach proposed in this study is feasible for reducing the area to be searched for illicit cannabis cultivation in semi-arid regions.

1. Introduction

Cannabis sativa is the most highly demanded illegal drug in the world, ahead of amphetamines, cocaine, and opiates (UNODC 2011). Although cannabis is considered to be a recreational drug in some countries (similar to alcohol and tobacco) (Murray et al. 2007), the consumption of this drug is prohibited in Brazil. One of the strategies employed

---

*Corresponding author. Email: alessandra.al@dpf.gov.br

to reduce its consumption is the identification and destruction of plantations. Although *C. sativa* is produced in at least 172 different countries, there is little information about the actual extent of its cultivation (Leggett and Pietschmann 2008), primarily because it is often cultivated at small scales (Hammersvick, Sandberg, and Pedersen 2012), in uninhabited regions (Lisita 2011), or even indoors (Carter 2009; Hurley, West, and Ehleringer 2010).

Traditionally, *C. sativa* fields in Brazil are identified by agents of the Brazilian Federal Police using helicopters and local knowledge acquired from previous missions (Lisita 2011). For example, *C. sativa* fields are primarily found near water sources (e.g. perennial or ephemeral rivers or ponds) and close to roads or trails. Identification of *C. sativa* fields is an expensive and time-consuming task that depends directly on the expertise and experience of police officers. At first glance, remotely sensed data would be efficient for detecting such fields because they are essentially multispectral, synoptic, repetitive, and cost effective. Such characteristics allow the discrimination of different targets on the Earth's surface (Jensen 2006). Daughtry and Walthall (1998) reported reflectance differences between *C. sativa* leaves and other representative leaves in the surrounding canopy in the green (550 nm), red (670 nm), red edge (720 nm), near-infrared (800 nm), and narrow (<30 nm) spectral bands. Pesaresi (2008) proposed the use of high-spatial resolution images (IKONOS) combined with textural analysis to detect terrains cultivated with coca plants in the Andean region.

Conventional pixel-per-pixel-based digital classification techniques of satellite images, primarily those using only single-date imagery, are generally of low efficiency in automatic pattern recognition, mainly because of variations in crop phenology, different cropping systems and heterogeneous measurement conditions during satellite overpasses (e.g. distinct atmospheric disturbances and solar illumination) (Vieira et al. 2012). In addition, most illegal *C. sativa* fields are found in small areas (farmers are concerned about their fields being found), there is no fixed crop calendar since producers use irrigation to plant throughout the year, and phenology information on local species is difficult to find in the literature. An alternative technique is the use of geographic, object-based image analyses (GEOBIA) (Hay and Castilla 2008; Blaschke 2010). According to Cohen and Shoshany (2005), conventional algorithms execute image processing guided only by statistical data variables, whereas GEOBIA encompasses computational systems based on knowledge. GEOBIA is based on image segmentation and construction of a hierarchical network of homogeneous objects. After an image is segmented, GEOBIA uses several types of data simultaneously to complete the image classification: pixel values, contextual information, object features, and neighbourhoods and hierarchical relationships, among others (Blaschke and Lang 2006; Peña-Barragán et al. 2011). In other words, GEOBIA considers not only the target's spectral information but also considers other features such as size and shape, or even surrounding characteristics.

A number of authors have highlighted the potential of GEOBIA to optimize the identification of complex targets using remotely sensed data (e.g. Gao et al. 2006; Durieux, Lagabrielle, and Nelson 2008; Nussbaum and Menz 2008; Whiteside, Boggs, and Maier 2011). As noted by Ratcliff (2010), *C. sativa* cultivation presents spatial characteristics that allow computer modelling. This study aimed to identify potential sites of *C. sativa* located in the semi-arid, southern part of Pernambuco State, Brazil, using object-based classification of Système Pour l'Observation de la Terre high resolution geometric (SPOT-5 HRG) images.

2. Approach

2.1. Study area

The study area corresponds to an area comprising approximately 2300 km^2 in the southern part of Pernambuco State, northeast Brazil, covered by a SPOT-5 scene (Figure 1). Fluvial islands found in the São Francisco River and hilly areas were excluded in the analysis because the *C. sativa* plantations in these areas present quite distinct spatial patterns from those observed in the predominantly flat landscape of the region. The test site includes the following municipalities: Cabrobó, Orocó, Belém de São Francisco, Salgueiro, and Terra Nova. The climate of this region is semi-arid. Vegetation is mainly represented by Caatinga physiognomies.
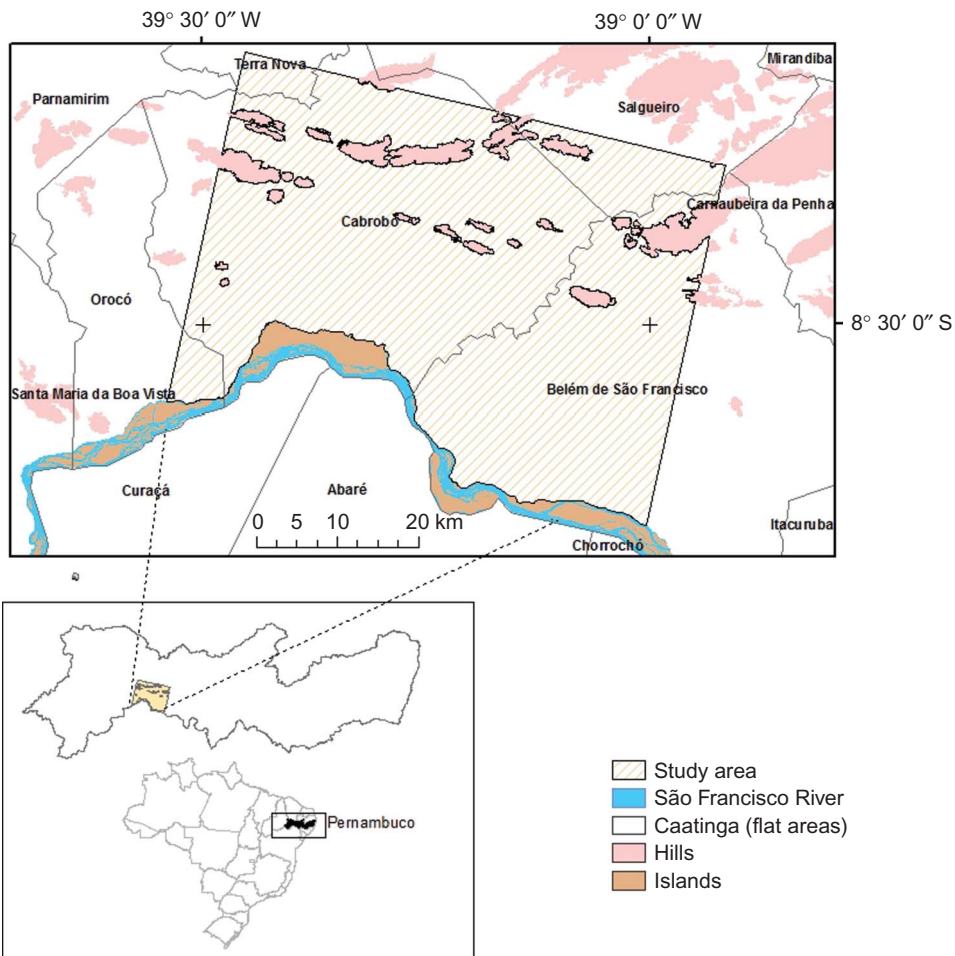

Figure 1.   Location of the study area in Pernambuco State, northeast Brazil. The study area corresponds to the municipalities of Cabrobó, Orocó, Belém de São Francisco, Salgueiro, and Terra Nova covered by the SPOT-5 HRG scene. Fluvial islands and hilly areas were excluded because the patterns of *Cannabis sativa* plantations in such areas are quite different from the predominantly flat landscape of the region.
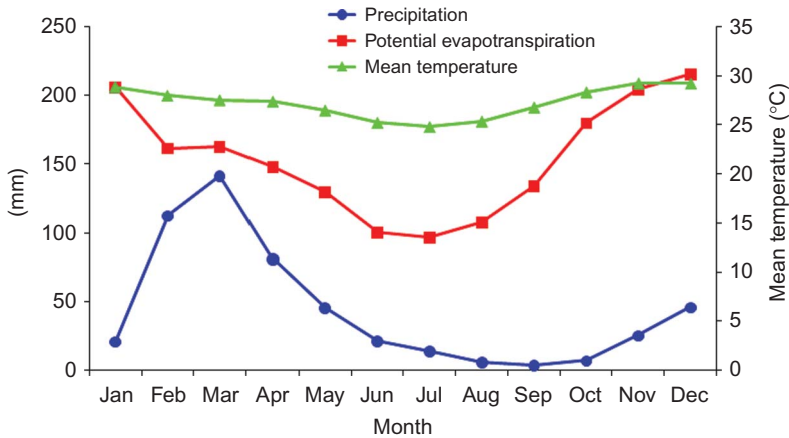
Figure 2. Typical temperature, precipitation, and potential evapotranspiration conditions in the study area, obtained from a meteorological station located in the Cabrobó municipality, Pernambuco State (latitude, 8.51° S; longitude, 39.33° W; elevation, 341.46 m; data set, 1 January 2000 to 31 December 2011). Potential evapotranspiration was estimated using the Thornthwaite approach. Water deficiency is found throughout the year, since potential evapotranspiration is higher than precipitation.

Typical temperature, precipitation, and potential evapotranspiration data of the study site are shown in Figure 2. Annual average temperature is 27.2°C, with a corresponding standard deviation of 1.6°C. Mean annual precipitation is ~520 mm, concentrated from February to April, while annual average potential evapotranspiration is ~1845 mm. The region faces water deficiency throughout the year, indicating the need for irrigation of *C. sativa*, regardless of planting date. Thus, cannabis producers from this region do not follow any crop calendar, making remote-sensing data interpretation more difficult because we often find variation in growing conditions of irrigated croplands regardless of dates of image acquisition.

C. sativa is an annual crop that can grow in most soil types, even in those of low soil fertility (Raman 1998). Greenhouse experiments conducted by Souza et al. (2006) showed a wide range of results in terms of shrub height (0.6–1.9 m). Ultimately, crop size is determined by environmental and management factors such as soil depth, solar radiation, and levels of fertilization and irrigation (Clarke 1981). In optimal conditions, *C. sativa* shrubs can reach a height of ~6 m during the 4–6 months of the growing season (Clarke 1981). However, the plant may face growth restriction if regrowth of native vegetation is not controlled (Raman 1998).

2.2. *Remote-sensing and ancillary data*

The remote-sensing data used as the basis for object-based classification comprised a SPOT-5 HRG multispectral image of 10 m spatial resolution and a panchromatic image of 2.5 m spatial resolution, acquired on 31 May 2007 (closest overpass in relation to the field campaign conducted by the Federal Police on 5–17 June 2007, as detailed below). SPOT-5 data were provided by the SEAS Guyane programme from the Institut de Recherche pour le Développement (IRD) in Cayenne, French Guiana.

Multispectral images were converted to surface reflectance using the FLAASH atmospheric correction package, which is a MODTRAN-4-based radiative transfer code

available in the Exelis ENVI^{TM} image processing software (Exelis, Boulder, CO, USA) (ITT 2009). The atmospheric model was set as tropical, the aerosol model was set as rural, initial visibility was set at 40 km, and the water vapour column multiplier was set at 0.7. The model was approximated by the equation $V = 3.912/\beta$, where V is visibility and β is the extinction coefficient (horizontal optical depth per km), derived by aerosol optical depth (AOD) divided by the effective aerosol thickness layer, which typically has a value of $\sim$2 km (ITT 2009). Parameters of AOD and water vapour were obtained from the Petrolina website, Aerosol Robotic Network (AERONET), Level 2.0, Quality Assured Data published by the National Aeronautics and Space Administration (NASA) Goddard Space Flight Center (GSFC).

Surface reflectance images were then converted into the normalized difference vegetation index (NDVI; Tucker 1979):

$$NDVI = \frac{\rho_{NIR} - \rho_{RED}}{\rho_{NIR} + \rho_{RED}}, \tag{1}$$

where ρ_{RED} is reflectance in the red wavelength (SPOT-5 band 2) and ρ_{NIR} is reflectance in the near-infrared wavelength (SPOT-5 band 3). Cloud cover-affected portions of the images ($\sim$26% of total area) were masked before image classification.

SPOT-5 HRG images from 1 July 2007 and 14 October 2007, which presented low cloud-cover conditions, were also analysed to generate basic vector layers of waterbodies (lakes and ponds) and land use (croplands, pasturelands, and urban areas). These two images were not considered in the image classification approach because of lack of field data close to the satellite overpasses to analyse classification performance.

Slope and stream networks were derived from Topodata (Valeriano and Rossetti 2012), which are Shuttle Radar Topography Mission (SRTM) data interpolated into a 30 m grid. To generate a basic streams map, we employed the hydrology tools available in the Spatial Analyst package of Environmental Systems Research Institute (ESRI) ArcGIS/Info 9.3.1. (Redlands, CA, USA) (ESRI 2010) adopting a minimum flow accumulation threshold of 50 (Jenson and Domingue 1988). First- and second-order streams were classified as ephemeral, and main streams were derived assuming a minimum flow accumulation threshold of 2000. Water source distance maps to lakes/ponds, streams/rivers, and ephemeral streams were derived from waterbodies, first- and second-order streams, and main streams on reference maps using distance tools available in the Spatial Analyst package (ESRI 2010).

2.3. *Field operation*

C. sativa fields were detected by aerial spotters during field operations conducted by the Brazilian Federal Police on 5–17 June 2007. According to records from the Cabrobó meteorological station, precipitation data were quite low over both time periods (5–17 June: 4.6 and 0.35 mm for total and average rainfall, respectively; 14–21 May: 0.6 and 0.08 mm, respectively). Field operations involved the acquisition of portable GPS coordinates and measurement of plant height and spacing. After the measurements had been completed, the plantations were destroyed. More detailed information about the location of the *C. sativa* sites was intentionally omitted due to the internal policies of the Brazilian Federal Police.

C. sativa size ranged from small seedlings to mature plants (Figure 3). Soil fertilization and irrigation are mandatory and were found at all sites visited. Growers use water from either natural or artificial water reservoirs (ponds, lakes, irrigation channels, perennial
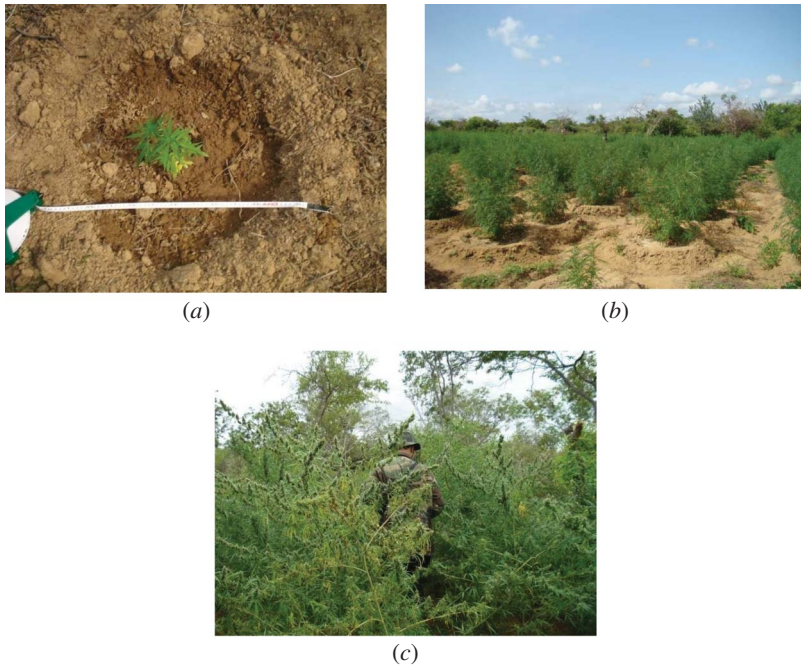
(*a*)

(*b*)

(*c*)

Figure 3.   *Cannabis sativa* plantations in the semi-arid region of Brazil at three different growing stages: initial (*a*), intermediate (*b*), and advanced (*c*).

streams, and runoff water from ephemeral streams stored during the rainy season). Because soils in this region are sandy (low water-holding capacity), a water supply in pits planted with *C. sativa* is provided daily by producers even when plants are mature (information based on field inspection).
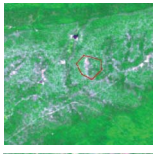
2.4.   Image processing and analysis

A vegetation density map of the study area was generated from the SPOT-5 HRG image using the supervised support vector machine (SVM) classification technique. SVM classifiers are based on machine learning and are considered to be a powerful method that often produces a higher classification accuracy than conventional classifiers (Mantero, Moser, and Serpico 2005; Pal and Mather 2005), even with limited training samples (Mountrakis, Im, and Ogole 2011).

The following classes were defined: very high-greenness vegetation, high-greenness vegetation, medium-greenness vegetation, low-greenness vegetation, very low-greenness vegetation, irrigated cropland/hygrophytes, waterbody, and bare soil. According to Huete et al. (2006), greenness of vegetation is a direct measurement of the photosynthetic potential of the canopy, and the intensity depends on total leaf chlorophyll, leaf area, canopy cover, and structure. In this study, the rationale for using different levels of greenness is that *C. sativa* crop management, including irrigation and nutrient supplies, results in distinct levels of photosynthetic activity as compared with that of the surrounding native vegetation. Training samples were collected in varying conditions of green cover and land use (Table 1).

Spectral patterns of *C. sativa* fields and other targets related to the fields were investigated through an analysis of the spectral profiles derived from a multi-temporal series of NDVI.

Table 1. Characteristics of training samples collected in varying conditions of green cover and land-use cover used in the OBIA-based image classification.

Class	Vegetation type	Number of pixels	Feature in the RGB/321 colour composite
Very high-greenness vegetation	Gallery forest	171	
High-greenness vegetation	Forested Caatinga	1712	
Medium-greenness vegetation	Arboreal Caatinga	1457	
Low-greenness vegetation	Shrub Caatinga	1280	
Very low-greenness vegetation	Caatinga grassland	1371	
Irrigated cropland/hygrophytes	Commercial cropland/humid natural grassland	1172	
Waterbody	–	5261	
Bare soil	–	359	

2.5. *Object-based image classification*

The object-based SPOT-5 HRG image classification was designed to detect alert features based on spatial and spectral patterns of *C. sativa* plantations and their surroundings. Object (segments) description employed fixed-threshold conditions and fuzzy logic membership functions. Input data sets to support the employment of contextual decision rules included thematic layers of vegetation greenness, waterbody, and bare soil classes generated using SVM, anthropogenic areas, and distance from waterbodies/streams.

Expert knowledge about typical spatial patterns (size and surrounding vegetation) related to *C. sativa* growing sites served as a basis for classification rule assignments. *C. sativa* plantations are usually small and cultivated within natural vegetation in order to make their identification more difficult from nearby roads. Thus, certain aspects in regard to maximum area and neighbourhood were considered in the identification of potential *C. sativa* cultivation. Spatial associations between *C. sativa* sites and different sources of water, investigated by Lisita (2011) through a weight of evidence approach (Bonham-Carter 1994), were also considered in the image classification.

Object-based classification was conducted by defining seven hierarchical scale levels resulting from segmentation/merging procedures. The first level comprised the segmentation of input layers and corresponding weights (Table 2; Figure 4). Image segmentation was based on a multiresolution segmentation algorithm available in the Trimble eCognition Developer software package (Munich, Germany; Trimble 2011). This algorithm employs the region-merging technique (Baatz 2000) to produce meaningful image objects as a first step for further classification and other processing procedures. The segmentation was performed by applying the standard parameters of scale, shape, and compact form (10, 0.1, and 0.5, respectively). Vector layers of masks for clouds and shadows and anthropogenic areas were also incorporated within the segmentation process.

In the segmentation process, the spatial resolution of the panchromatic image (2.5 m) played an important role in defining the limits of targets, while the four bands of SPOT-5 HRG multispectral images, NDVI, and SVM raster were integrated to distinguish between different spectral classes. Although the raster layers of slope, distance from lakes and ponds, distance from streams/rivers, and distance from ephemeral streams were not weighted in

Table 2. Segmentation weights of input layers used in OBIA.

Layer	Description	Weight/thematic layer usage
1	SPOT-5 HRG Band 1	1
2	SPOT-5 HRG Band 2	1
3	SPOT-5 HRG Band 3	1
4	SPOT-5 HRG Band 4	1
5	NDVI	2
6	SPOT-5 PAN	2
7	Slope	0
8	SVM classes	1
9	Distance from lakes/ponds	0
10	Distance from streams/rivers	0
11	Distance from ephemeral streams	0
T1	Anthropogenic areas	Yes
T2	Masked clouds/shadows	Yes

Notes: Layers with weight = 0 were used in the image classification but had no influence on image segmentation. 'Yes' signifies that the boundaries of polygons contributed to the segmentation. Layers T1 and T2 correspond to binary vector maps, where value = 0 means unclassified and value = 1 means anthropogenic area and clouds/shadows.
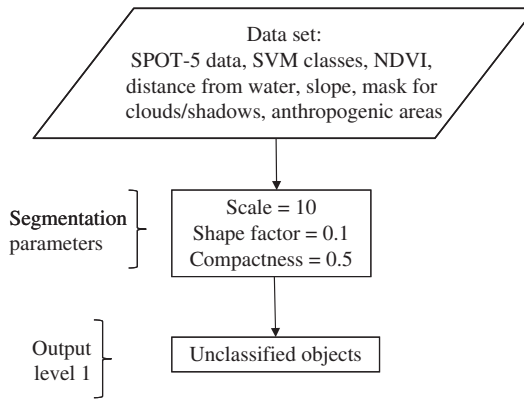
Figure 4.   Flowchart of level 1 object-based image classification (segmentation).
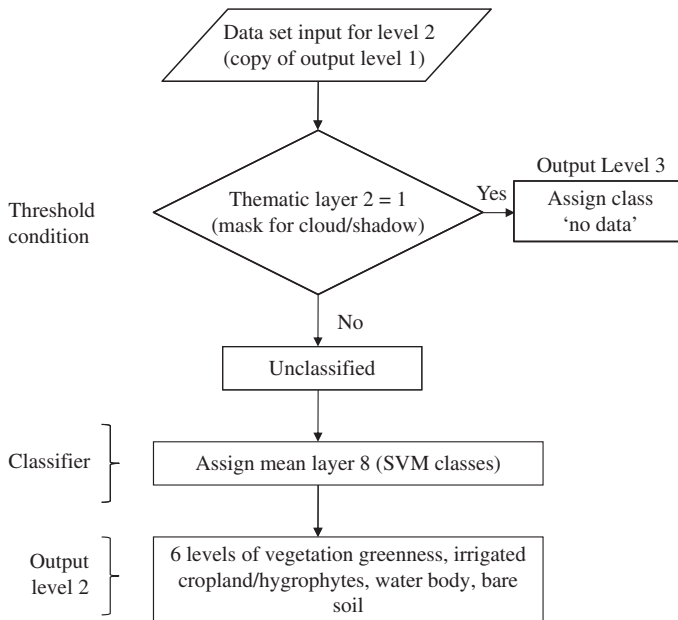
Figure 5.   Flowchart of level 2 object-based image classification (discrimination of six classes of vegetation greenness, irrigated cropland/hygrophytes, waterbody, bare soil, and clouds/shadows).

the segmentation, the thematic attributes provided by those layers were assigned to image objects created in the segmentation to allow the use of that information during the following steps of the classification process.

In the first step (Figure 5), we employed a threshold condition for vector thematic layer 2, at level 2 (T2 value in Table 2 equal to 1) to flag clouds and shadows as no data. Next, the vegetation greenness, irrigated cropland/hygrophytes, waterbody, and bare soil classes resulting from previous SVM classification (layer 8) were assigned to corresponding remaining image objects using a membership function. The objective of this component was to incorporate the results from a powerful per-pixel-based classification to effectively discriminate relevant spectral classes.
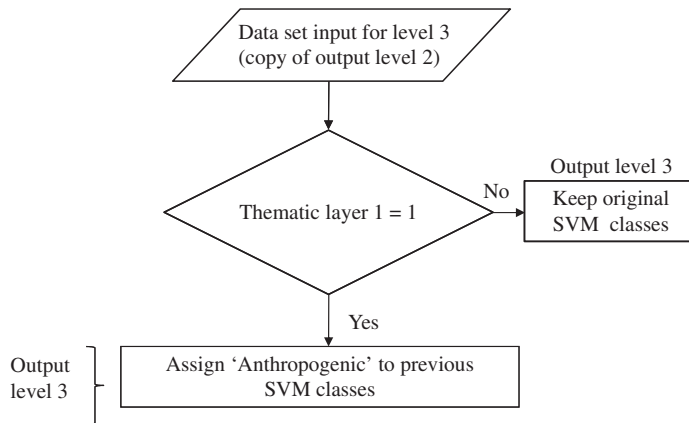
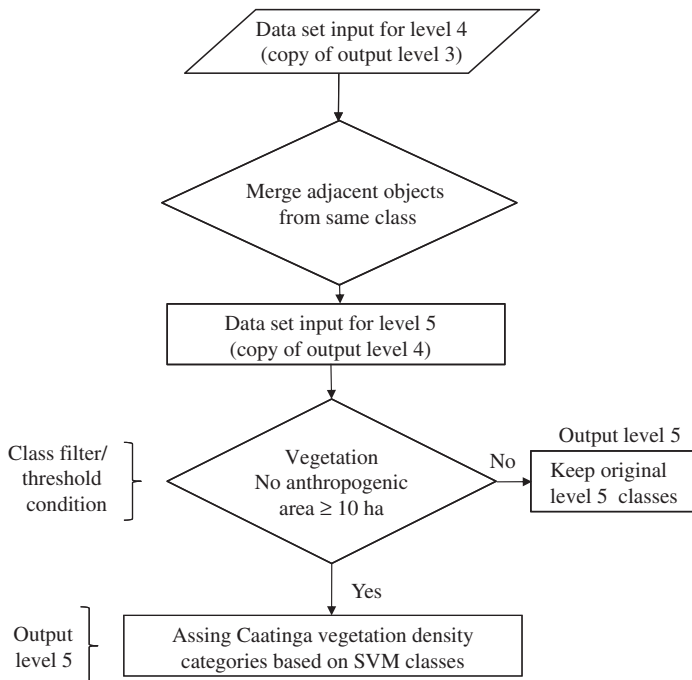Figure 6. Flowchart of level 3 object-based image classification (assignment of anthropogenic classes).

Figure 7. Flowchart of levels 4 and 5 object-based image classification (assignment of Caatinga vegetation density categories).

Classification of anthropogenic areas (scale level 3) was the next step (Figure 6). Here, we employed ancillary data to classify anthropogenic areas. Those objects from the previous step that satisfied the threshold condition 'thematic layer 1 = 1' were assigned to the class named anthropogenic. In order to generate a higher scale level (scale levels 4 and 5), adjacent objects from the same class were merged. Then, considering that, regionally, homogeneous vegetation occupying huge areas usually corresponds to
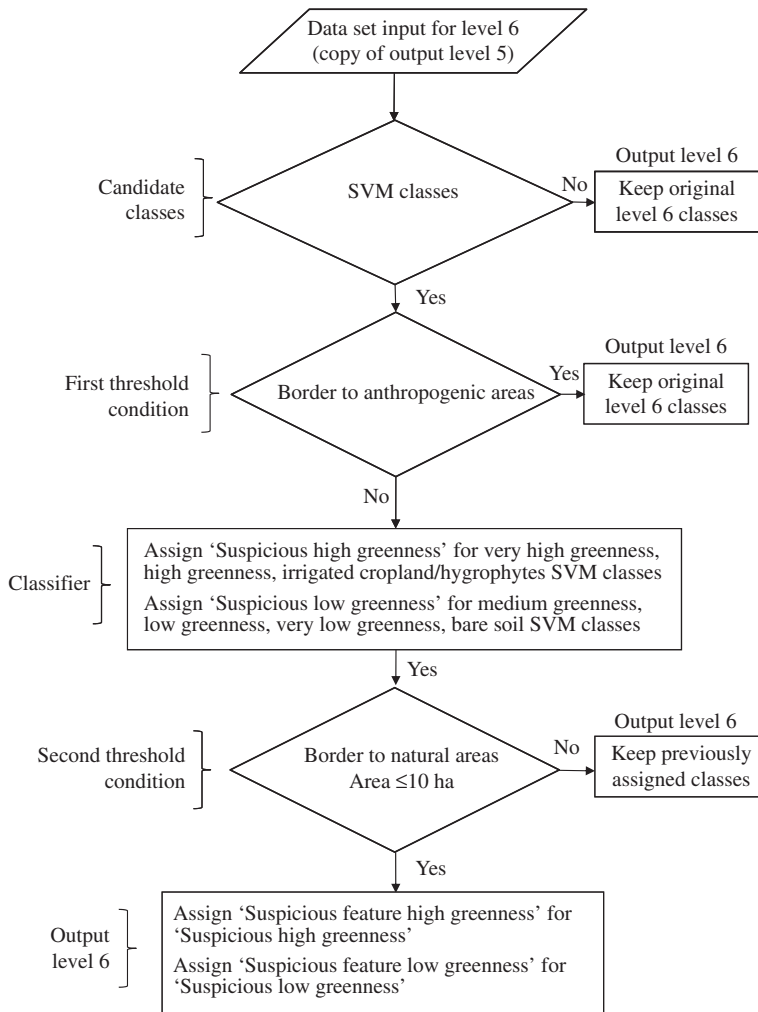
Figure 8. Flowchart of level 6 object-based image classification (assignment of suspicious feature categories).

natural Caatinga physiognomies, we employed a class filter and a minimum size threshold condition to classify image objects into Caatinga density categories (Figure 7).

For the classification of 'suspicious features' (scale level 6) (Figure 8), we classified contrasting small objects surrounded by natural vegetation as 'suspicious features', assuming that they presented spectral, geometrical, and neighbourhood patterns coherent with *C. sativa* fields. In the first step, we employed a border to anthropogenic areas threshold condition to classify candidate image objects (non-anthropogenic, non-natural cover) as 'suspicious'. The image objects that satisfied the aforementioned threshold condition were classified into either suspicious high greenness (assigned to image objects derived from very high-greenness vegetation, high-greenness vegetation, or irrigated croplands/hygrophytes classes) or suspicious low greenness (assigned to image objects derived from medium-greenness vegetation, low-greenness vegetation, very low-greenness vegetation, and bare soil objects). Next, we employed a threshold condition of border to

natural areas and maximum size to assign the classes 'suspicious features high greenness' and 'suspicious features low greenness'.

Maximum-alert classes (ponds, perennial streams/ephemeral streams) (scale level 7) (Figure 9) were assigned to image objects classified as suspicious features (high greenness) that satisfied the specific criteria of maximum distance from waterbodies (value of layers 9, 10, and 11). High-alert classes (ponds, perennial streams/ephemeral streams) were assigned to image objects classified as suspicious features (low greenness) that satisfied the specific criteria of maximum distance from waterbodies (value of layers 9, 10, and 11). The last level included, besides all the classes from the lower level, high-alert (possible cultivation at the beginning of the growing season), and maximum-alert (possible cultivation during the peak of the growing season) classes.

The results of object-based image classification were verified using the weight of evidence technique available in the ArcSDM (Spatial Data Modeller) algorithm (Spatial
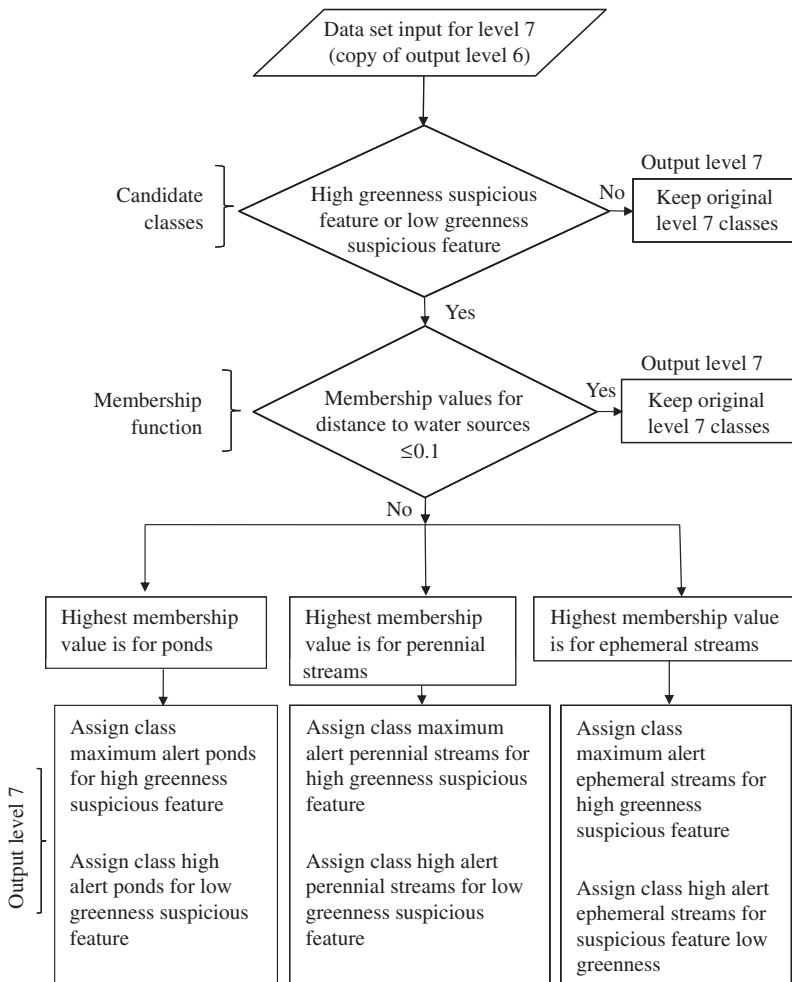

Figure 9. Flowchart of level 7 object-based image classification (assignment of maximum-alert and high-alert categories).

Analyst Package, ESRI ArcGIS 9.3.1 software) (Sawatzky et al. 2004). We used the categorical method and T (studentized contrast) = 2 (approximately 98% of probability). The training areas corresponded to 15 previously known *C. sativa* sites identified during the police operation conducted on 5–17 June 2007. After the weights of evidence were calculated, we analysed the values of weights, W+, W−, and contrast, CNT, for different classes.

3. Results

The mean spectral profiles of greenness-related training samples selected for the SVM classification are shown in Figure 10. More significant 'green' photosynthetic signals for classes of higher greenness are represented in the figure by higher absorption in the visible, higher reflectance in near-infrared and decreasing reflectance in shortwave infrared. Classes of lower greenness show increasing contribution of the soil signal through increased reflectance in the visible and other wavebands. Very high greenness shows a subtle reduction in albedo when compared with high greenness, which could be attributed to canopy effects in a woody-dominated physiognomy.

The OBIA results are summarized in Table 3. Features corresponding to the maximum-alert features related to lake, perennial streams, and ephemeral streams (membership value >0.9) are presented in Figures 11, 12, and 13, respectively. Regarding the last case, it is important to point out that alerts should be considered only when streams present sufficient water for irrigation.

Examples of *C. sativa* sites located following police field operations conducted on 5–17 June 2007 and classified as maximum-alert features are presented in Figures 14 and 15. Among the 15 *C. sativa* sites identified during the police operation during that month (and located in the SPOT-5 HRG scene), eight were classified as maximum alert (total area of maximum-alert class = 22.54 km^2). The classification system detected more than 50% of known *C. sativa* sites, showing a high predictive power for the classification.
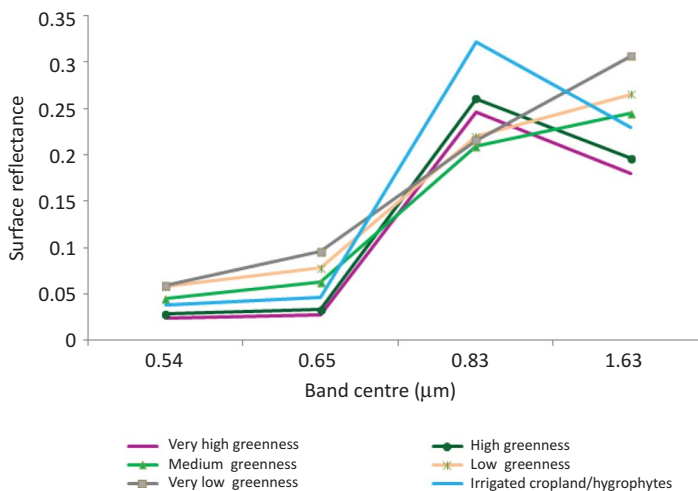

Figure 10. Spectral profiles of training sites (discriminated based on the intensity of greenness) used in the supervised classification of SPOT-5 HRG scenes from 31 May 2007 by the support vector machine (SVM) classifier.

Table 3. Results of *Cannabis* feature detection in SPOT-5 HRG image (overpass: 31 May 2007) through analysis of weights of evidence.

No.	Class	Area (km²)	n	W+	S_W+	W−	S_W−	CNT	CNT (S)	STUD.CNT	G	W	W_STD
1	Generic	134.83	0	0	0	0	0	0	0	0	99	−0.75	0.38
2	Anthropogenic	244.16	0	0	0	0	0	0	0	0	99	−0.75	0.38
7	Water	21.83	0	0	0	0	0	0	0	0	99	−0.75	0.38
8	Forest	0.26	0	0	0	0	0	0	0	0	99	−0.75	0.38
9	Suspicious features (low greenness)	80.68	0	0	0	0	0	0	0	0	99	−0.75	0.38
10	Suspicious features (high greenness)	53.94	1	0.80	1.00	−0.04	0.27	0.84	1.04	0.81	99	−0.75	0.38
20	Forested Caatinga	326.78	0	0	0	0	0	0	0	0	99	−0.75	0.38
21	Arboreal Caatinga	522.53	3	−0.37	0.58	0.12	0.29	−0.49	0.65	−0.76	99	−0.75	0.38
22	Shrub Caatinga/pasture	92.96	0	0.00	0.00	0.00	0.00	0.00	0.00	0.00	99	−0.75	0.38
23	Caatinga grassland/pasture	150.37	1	−0.22	1.00	0.02	0.27	−0.24	1.04	−0.23	99	−0.75	0.38
24	Suspicious (high greenness)	37.36	1	1.17	1.00	−0.05	0.27	1.22	1.04	1.17	99	−0.75	0.38
25	Suspicious (low greenness)	89.03	1	0.30	1.00	−0.02	0.27	0.32	1.04	0.31	99	−0.75	0.38
26	Maximum alert (ponds)	5.45	3	4.20	0.58	−0.22	0.29	4.42	0.65	6.83	26	4.20	0.58
27	Maximum alert (perennial streams)	7.79	3	3.84	0.58	−0.22	0.29	4.06	0.65	6.28	27	3.84	0.58
28	Maximum alert (temporary streams)	9.30	2	3.25	0.71	−0.14	0.28	3.39	0.76	4.46	28	3.25	0.71
29	High alert (ponds)	5.16	0	0	0	0	0	0	0	0	99	−0.75	0.38
30	High alert (perennial streams)	6.99	0	0	0	0	0	0	0	0	99	−0.75	0.38
31	High alert (temporary streams)	12.65	0	0	0	0	0	0	0	0	99	−0.75	0.38
	Total	1802	15										

Notes: We used information on *Cannabis sativa* fields found during the operation of June 2007, categorical method, and T (studentized contrast) = 2 (approximately 98% of probability). *n* is number of *C. sativa* fields located in respective class; W+ and W− are positive and negative weights; S_W+ and S_W− are positive and negative weights standard deviations. CNT, contrast; STUD.CNT, studentized contrast; *G* = generalized class (a generalized value of 99 is assigned to classes that do not meet the confidence criteria); *W* = weight; W_STD = weight standard deviation.
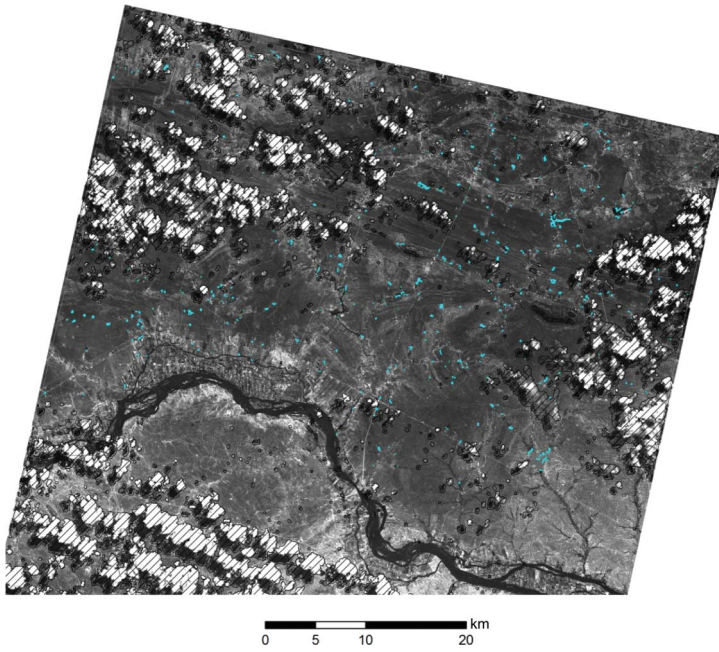
Figure 11.   Maximum alerts yielded by object-based image classification and related to lakes (coloured blue). Image corresponds to the SPOT-5 colour composite of 31 May 2007.
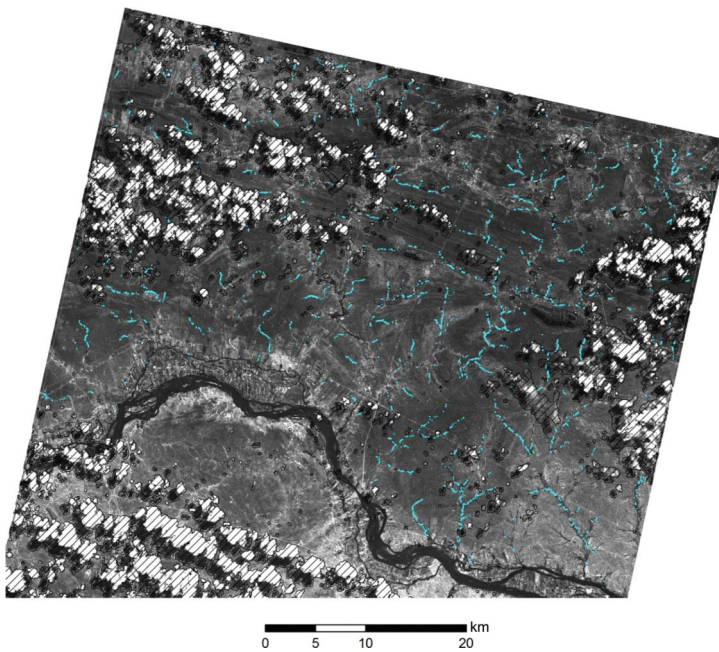

Figure 12.   Maximum alerts yielded by object-based image classification and related to perennial streams (coloured blue). Image corresponds to the SPOT-5 colour composite of 31 May 2007.
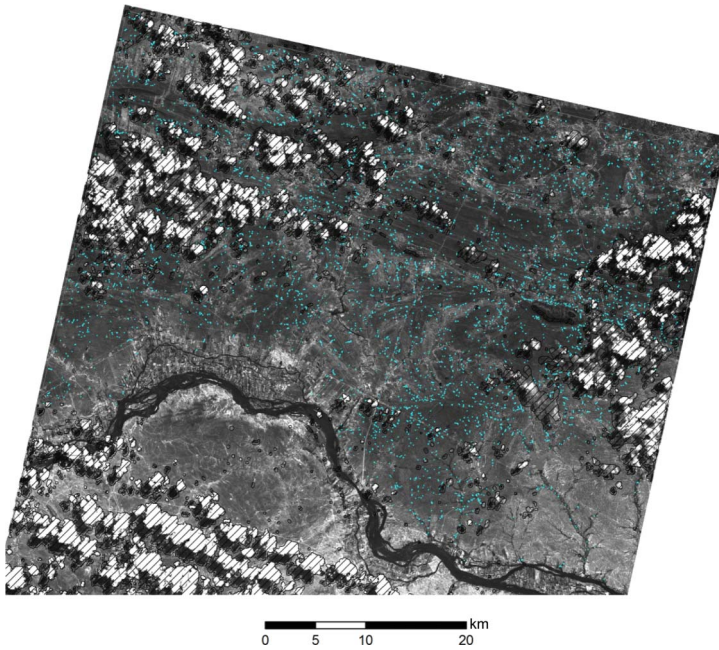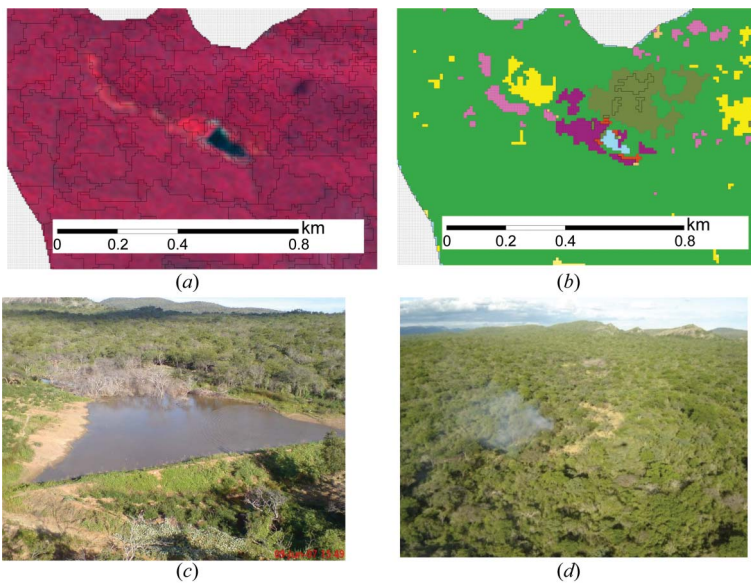
Figure 13.   Maximum alerts yielded by object-based image classification and related to ephemeral streams (coloured blue). Image corresponds to the SPOT-5 colour composite of 31 May 2007.
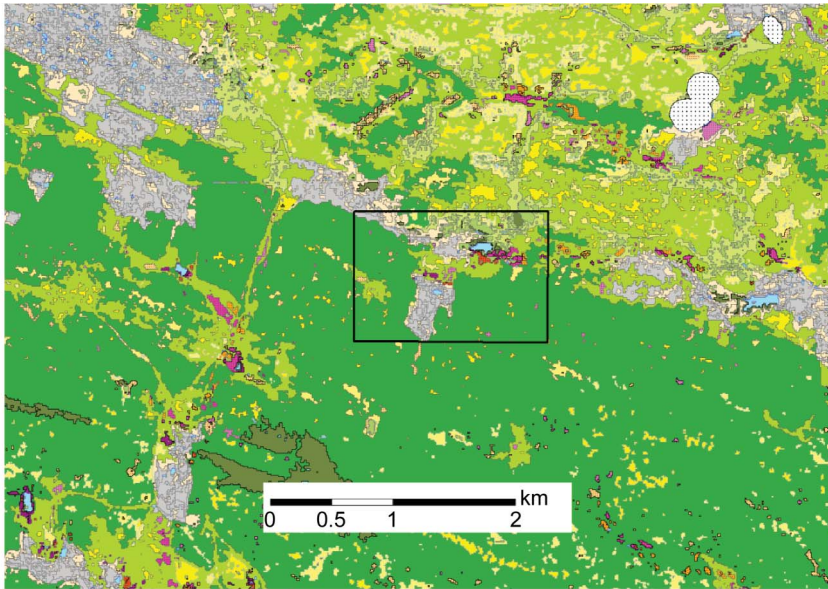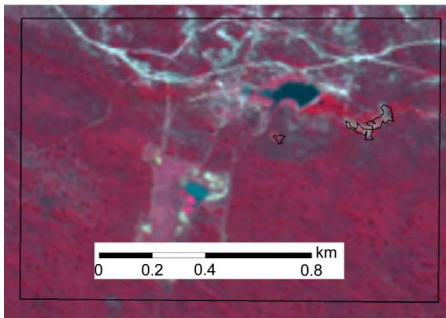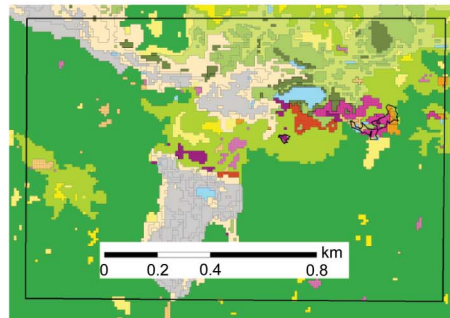

Figure 14.   Segmentation result (*a*) and object-oriented classification (*b*) of SPOT-5 HRG scene (overpass: 31 May 2007), highlighting segments corresponding to plantations of *Cannabis sativa* confirmed in the field campaign. Pink- and purple-dotted segments correspond to maximum alert identification. Images (*c*) and (*d*) are panoramic views of *C. sativa* cultivation obtained by helicopter in a field campaign conducted on 9 June 2007. Photographs: Brazilian Federal Police.

Figure 15. Subset of object-based image (SPOT-5 HRG, overpass: 31 May 2007) classification result (*a*); (*b*) detail of SPOT-5 HRG scene (overpass: 31 May 2007), highlighting GPS tracks (in black) corresponding to plantations of *Cannabis sativa* confirmed in the field campaign conducted during June 2007 and classified as having maximum alert features (*c*) through OBIA.

Results of the classification selected an excessive number of features classified as alert (commission error), demanding a subsequent step of visual editing to obtain more feasible results. This was part of the strategy of the study since, for tactical purposes, it is preferable to have more commission errors than omission errors.

4. Conclusions

(1) An object-oriented image classification allowed a semi-automatic detection of features common to *C. sativa* plantations in the SPOT-5 images through the combination of spatial and spectral patterns in the classification process.
(2) The proposed classification was based on logical arguments rather than a trial-and-error process, which makes the methodology easier to replicate. The classification rules can be employed in similar conditions for different data sets, requiring the preparation of input layers.
(3) The results showed that the approach proposed in this study is feasible for identifying potential areas of *C. sativa* cultivation in semi-arid regions and on a regional scale. To some extent, the method can be adapted to other regions with similar challenges.

Acknowledgements

References

Baatz, M. 2000. "Multiresolution Segmentation: An Optimization Approach for High Quality Multi-Scale Image Segmentation." *Journal of Photogrammetry and Remote Sensing* 58: 12–23.
Blaschke, T. 2010. "Object-Based Image Analysis for Remote Sensing." *ISPRS Journal of Photogrammetry and Remote Sensing* 65: 2–16.
Blaschke, T., and S. Lang. 2006. "Object-based Image Analysis for Automated Information Extraction – A Synthesis." In *Proceedings of the MAPPS/ASPRS 2006 Falls Conference*, San Antonio, Texas, November 6–10, 2006. Accessed April 30, 2012. http://ispace.researchstudio.at/downloads/2006/173_full.pdf.
Bonham-Carter, G. F. 1994. *Geographic Information Systems for Geoscientists: Modelling with GIS*, 398p. Ontario: Pergamon Press.
Carter, C. 2009. "Making Residential Cannabis Growing Operations Actionable: A Critical Policy Analysis." *International Journal of Drug Policy* 20: 371–376.
Clarke, R. C. 1981. *Marijuana Botany. An Advanced Study. The Propagation and Breeding of Distinctive Cannabis*, 220p. Oakland: Ronin.
Cohen, Y., and Shoshany, M. 2005. "Analysis of Convergent Evidence in an Evidential Reasoning Knowledge-Based Classification." *Remote Sensing of Environment* 96: 518–528.
Daughtry, C. S. T., and C. L. Walthall. 1998. "Spectral Discrimination of *Cannabis Sativa L*. Leaves and Canopy." *Remote Sensing of Environment* 64: 192–201.
Durieux, L., E. Lagabrielle, and A. Nelson. 2008. "A Method for Monitoring Building Construction in Urban Sprawl Areas Using Object-Based Analysis of SPOT 5 Images and Existing GIS Data." *International Journal of Photogrammetry and Remote Sensing* 63: 399–408.

ESRI. 2010. *What's New in ArcGIS10*, 177p. Redlands, CA: ESRI.

Gao, Y., J. F. Mas, B. H. P. Maathius, Z. Xiangmin, and P. M. Van Dijk. 2006. "Comparison of Pixel-Based and Object-Oriented Image Classification Approaches – A Case Study of a Coal Fire Area, Wuda, Inner Mongolia, China." *International Journal of Remote Sensing* 27: 4039–4055.

Hammersvick, E., S. Sandberg, and W. Pedersen. 2012. "Why Small-Scale Cannabis Growers Stay Small: Five Mechanisms That Prevent Small-Scale Growers from Going Large Scale." *International Journal of Drug Policy* 23: 458–464.

Hay, G. J., and G. Castilla. 2008. "Object-based Image Analysis." In *Spatial Concepts for Knowledge-Driven Remote Sensing Applications*, edited by T. Blaschke, G. Hay, and S. Lang, 75–89. Berlin: Springer.

Huete, A. R., K. F. Huemmrich, T. Miura, X. Xiao, K. Didan, W. Van Leeuwen, F. Hall, and C. J. Tucker. 2006. "Vegetation Index Greenness Global Dataset." White Paper for NASA ESDR/CDR. Accessed May 12, 2012. http://cce.nasa.gov/mtg2008_ab_presentations/VI_Huete_whitepaper.pdf

Hurley, J. M., J. B. West, and J. R. Ehleringer. 2010. "Tracing Retail Cannabis in the United States: Geographic Origin and Cultivation Patterns." *International Journal of Drug Policy* 21: 222–228.

ITT. 2009. *Atmospheric Correction Module: QUAC and FLAASH User's Guide.* Version 4.7., 44p. Boulder, CO: ITT Visual Information Solutions. http://www.exelisvis.com/portals/0/pdfs/envi/Flaash_Module.pdf

Jensen, J. R. 2006. *Remote Sensing of the Environment: An Earth Resource Perspective*. 2nd ed., 608p. Upper Saddle River, NJ: Prentice Hall.

Jenson, S. K., and J. O. Domingue. 1988. "Extracting Topographic Structure from Digital Elevation Data for Geographic Information System Analysis." *Photogrammetric Engineering and Remote Sensing* 54: 1593–1600.

Leggett, T., and T. Pietschmann. 2008. "A Cannabis Reader. Global Issues and Local Experiences." In *Monograph Series 8*, edited by R. Sznitmann, B. Olsson, and R. Room, 189–212. Lisbon: European Monitoring Centre for Drugs and Drug Addiction.

Lisita, A. 2011. "Semi-automated Mapping of Illicit *Cannabis Sativa* Cultivations in the Semi-arid Region of State of Pernambuco Through Data Integration of SPOT5 HRG Images, Ancillary Geographical Data and Field Knowledge." PhD diss., University of Brasília, Brasília, 210p. (in Portuguese).

Mantero, P., G. Moser, and S. B. Serpico. 2005. "Partially Supervised Classification of Remote Sensing Images Through SVM-Based Probability Density Estimation." *IEEE Transactions on Geoscience and Remote Sensing* 43: 559–570.

Mountrakis, G., J. Im, and C. Ogole. 2011. "Support Vector Machines in Remote Sensing: A Review." *ISPRS Journal of Photogrammetry and Remote Sensing* 66: 247–259.

Murray, R. M., P. D. Morrison, C. Henquet, and M. Di Forti. 2007. "*Cannabis*, the Mind and Society: The Harsh Realities." *Nature* 8: 885–895.

Nussbaum, S., and G. Menz. 2008. *Object-Based Image Analysis and Treaty Verification: New Approaches in Remote Sensing Applied to Nuclear Facilities in Iran*, 170p. Berlin: Springer.

Pal, M., and P. M. Mather. 2005. "Support Vector Machines for Classification in Remote Sensing." *International Journal of Remote Sensing* 26: 1007–1011.

Peña-Barragán, J. M., M. K. Ngugi, R. E. Plant, and J. Six. 2011. "Object-Based Crop Identification Using Multiple Vegetation Indices, Textural Features and Crop Phenology." *Remote Sensing of Environment* 115: 1301–1316.

Pesaresi, M. 2008. "Textural Analysis of Coca Plantations Using Remotely Sensed Data with Resolution of 1 Metre." *International Journal of Remote Sensing* 29: 6985–7002.

Raman, A. 1998. "The Cannabis Plant: Botany, Cultivation and Processing for Use." In *Cannabis - The Genus Cannabis*, edited by D. T. Brown, 29–54. Amsterdam: Harwood Academic Publishers.

Ratcliff, J. H. 2010. "Crime Mapping. Spatial and Temporal Challenges." In *Handbook of Quantitative Criminology,* edited by A. R. Piquero and D. Weisburd, 5–24. New York: Springer Science and Business Media.

Sawatzky, D. L., G. L. Raines, G. F. Bonham-Carter, and C. G. Looney. 2004. "ARCSDM3.1: ArcMAP Extension for Spatial Data Modeling Using Weights of Evidence, Logistic Regression, Fuzzy Logic and Neural Network Analysis." Accessed August 12, 2011. http://www.ige.unicamp.br/sdm/ArcSDM31/default_e.htm

Souza, D. Z., K. Michelin, M. G. Holler, G. L. G. Soares, M. R. Ritter, and N. R. Bianchi. 2006. "Roteiro Ilustrado Para Identificação Morfológica de *Cannabis sativa* L." *Perícia Federal* 24: 16–22.

Trimble. 2011. *eCognition Developer 8.64.1-User Guide*, 242p. Munchen: Trimble Germany GmbH.

UNODC. 2011. *World Drug Report 2011*. United Nations Publication, Sales No: E.11.XI.10. Accessed March 16, 2011. http://www.unodc.org/documents/data-and-analysis/WDR2011/World_Drug_Report_2011_ebook.pdf

Valeriano, M. M., and D. F. Rossetti. 2012. "Topodata: Brazilian Full Coverage Refinement of SRTM Data." *Applied Geography* 32: 300–309.

Vieira, M. A., A. R. Formaggio, C. D. Renno, C. Atzberger, D. A. Aguiar, and M. P. Mello. 2012. "Object-based Image Analysis and Data Mining Applied to a Remotely Sensed Landsat Time-series to Map Sugarcane over Large Areas." *Remote Sensing of Environment* 123: 553–562.

Whiteside, T. G., G. S. Boggs, and S. W. Maier. 2011. "Comparing Object-based and Pixel-based Classifications for Mapping Savannas." *International Journal of Applied Earth Observation and Geoinformation* 13: 884–893.